

UNIVERSITY OF CENTRAL OKLAHOMA  
Edmond, Oklahoma  
Jackson College of Graduate Studies & Research

**Primary Motor Cortex Stimulation Facilitates Visual Guidance**


A THESIS  
SUBMITTED TO THE GRADUATE FACULTY  
in partial fulfilment of the requirements  
for the degree of  
MASTER OF ARTS IN EXPERIMENTAL PSYCHOLOGY

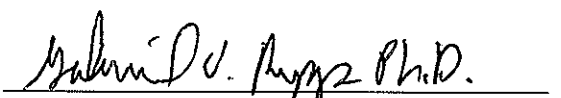
By  
Thomas C. Taylor  
Edmond, Oklahoma  
2015


**Primary Motor Cortex Stimulation Facilitates Visual Guidance**

A THESIS  
APPROVED FOR THE DEPARTMENT OF PSYCHOLOGY

2015

BY   
Mickie Vanhoy, Ph.D. Committee Chair

  
Gabriel Rupp, Ph.D. Committee Member

  
Wayne Ford, Ph.D. Committee Member

## Acknowledgments

Special Thanks to all the people who helped along the way,  
Including the Office of Research and Grants at UCO for funding and support,  
The College of Education and Professional Studies for the lab space and travel funding,  
The Jackson School of Graduate Studies and the Psychology Department,

My thesis advisory committee for guidance and sanity,

Advisor: Vanhoy, M., Ph.D.

Rupp, G., Ph.D.

Lord, W., PhD.

Aaron Likens for the MF DFA knowledge and coding support,

Adam Braly for the massive python coding stent,

My Research Assistants,

ShanShan Huang

JingJing Wang

Hunter Klevguard

And all the others around the lab.

Primary Motor Cortex Stimulation Facilitates Visual Guidance

Thomas C. Taylor

University of Central Oklahoma

### **Abstract**

The choices for analyzing cognitive load performance data are often problematic as they are task-dependent and do not generalize well. This makes research into task-independent variables necessary. Complexity is one such measure that one can retrieve from normal cognitive load measurements. Using time series analysis techniques provides an efficient, less altered route to measurements that can account for multiple task-dependent measures without being attached to the specific task. In this experiment, we present stimuli to participants based on occluded hand location to determine object recognition effectiveness. Maintaining a 65%- 75%-correct identification rate using a staircase procedure allowed for object recognition time and accuracy profile creation. Over the 18-inch hand movement, we observed a bimodal distribution in reaction times with a “far hand effect” decreasing times at around 18-15 inches from the stimulus, increasing to a peak at 15-12 inches, and decreasing again as a participant moves his/her hand closer to the stimulus. Nonlinear time series analysis was performed on the data; more specifically I used wavelet transform modulus maxima to analyze a continuous wavelet transform created from the time series based off the effect hand location has on object perception.

Keywords: Covert attention, embodied cognition, guidance, near-hand effect.

## TABLE OF CONTENTS

I.	Conceptualizing mental effort .....	5
	A. Cognitive load and task difficulty .....	5
	B. Operationalizing task difficulty as task complexity .....	6
II.	Factors in task difficulty .....	7
	A. Dual task.....	8
	B. Increase novelty/unpredictability.....	8
	C. SOA .....	8
III.	Performance indicators of task difficulty .....	9
	A. RT .....	9
	B. Accuracy .....	10
	C. Limitations .....	10
	D. An alternative .....	11
IV.	Time Series analyses .....	11
	A. Pre-whitening.....	12
	B. Smoothing. ....	13
	C. Representation. ....	15
	D. Decomposition. ....	16
V.	Wavelet Transform Modulus Maxima .....	17
	A. Wavelets and scales .....	17
	B. Iterations and correlations .....	18
	C. Maxima and singularities .....	20
	D. Measuring the System .....	21
	1. Hurst .....	22
	2. Holder .....	22
	3. Fractal Dimension .....	22
	4. Multifractal spectra.....	23
	E. Self-organization of performance .....	24
	1. Replication of near-hand effect .....	24
	2. More subtle effects .....	25
VI.	Method .....	25
	A. Participants .....	25
	B. Materials .....	26
	C. Procedure.....	27
	D. Data Analysis.....	29
	1. Separation into blocks.....	29
	2. Pre-whitening.....	31
	3. Decomposition into wavelets.....	32
	4. Iterations and correlations.....	32
	5. Maxima and singularities.....	32
	6. Holder exponents.....	33
VII.	Results.....	33
	A. Near hand effect.....	33
	B. Overall task complexity.....	34
	1. Task complexity across participants.....	34
	C. Multifractal spectra .....	36

VIII.	Discussion.....	40
	A. Replication of near-hand effect.....	40
	B. Self-organization of performance.....	40
	1.SOA as index of performance.....	41
	C. Multifractal spectra as task-independent measure of complexity.....	41
	1.Holder.....	41
	2. Self-Organized Criticality.....	42
	D. Task difficulty operationalized as task complexity.....	42
	E. Cognitive load re-conceptualized as task complexity.....	42
	F. Broader impacts.....	43
IX.	References.....	44
X.	Appendix A.....	49
XI.	Thesis Summary Document.....	50

## Primary Motor Cortex Stimulation Facilitates Visual Guidance and Attention

### **Conceptualizing mental effort**

#### **Cognitive load and task difficulty.**

Conceptually, cognitive load is the strain put on mental mechanisms during performance or schema creation. Several factors interfere with one's task performance in the form of cognitive load. Cognitive load conceptually stems from problem solving studies involving working memory models (Sweller, 1988). People are unable to delegate effective cognitive ability levels to secondary responsibilities when performing intensive primary task, presumably due to the increased load reducing the participant's schema-forming effectiveness. In an effort to assist others in reducing extraneous variables in studies, researchers have differentiated cognitive load into three basic categories: intrinsic, extraneous, and germane (DeLeeuw & Mayer, 2008).

Intrinsic cognitive load is the inherent amount of difficulty associated with a specific topic (Chandler & Sweller, 1991). Time series analysis, for example, requires combinations of mathematical and computer programming knowledge. Both these topics are inherently difficult to learn. Combining the tasks introduces an exponential increase in difficulty. Reducing intrinsic cognitive load requires one to break the task up into sub-tasks. Given the above example, one could start by learning why a time series differs from regular data and add to his/her schemas from there. This process allows for eventual mastery of multiple difficult tasks and the ability to combine schemas in new and unique ways that previously would not have been possible. Controlling for this cognitive load type requires practice rounds, allowing the participant to pre-form the schema required for the task one wishes to perform.



Extraneous cognitive load refers to how instructors represent information or tasks to a learner (Chandler & Sweller, 1991). Giving poor instructions to perform a difficult task results in a substantial increase in task complexity and results in increased cognitive load (Ginns, 2006). Reducing this cognitive load type, particularly by relating it spatially or temporally to another existing schema, allows for greater information consumption and task performance. One can see this effect when looking at various ways to describe a wavelet one used in a transform. Using the mathematical formula and performing advanced scaling techniques numerically on paper requires more effort on the learner's behalf than showing them the concept pictorially. Proper metaphor use can often avoid this issue, but if one is speaking to people from multiple cultures this confound can increase difficulty in finding appropriate allegories.

Germane cognitive load is the load devoted to processing, construction, and automation of schemas. The ability to remove completely this cognitive load type through any methods does not currently exist, making it the ideal task efficiency measurement. The best way to improve learning, until recently, was to reduce intrinsic and extraneous cognitive load (Sweller, Merrienboer, & Paas, 1998). Various techniques make it possible now to redirect both intrinsic and extraneous cognitive load into germane load, increasing the schema formation and learning rate.

### **Operationalizing task difficulty as task complexity.**

Researchers often give people a repetitive task and measure the decline in performance as task difficulty increases to study cognitive load. By allowing germane cognitive load to fall to a baseline, and minimizing any intrinsic or extraneous cognitive load through practice techniques before data collection begins, researchers can correlate in-

creases in cognitive load to task complexity through increased latency (Paas, Van Merriënboer, & Jeroen, 1993). This approach was further verified in research involving memory sequencing in various cognitive load situations (Robinson, 2001).

### **Factors in task difficulty.**

Heavy cognitive load has negative task performance effects, no matter the type, and the cognitive load experience differs from person to person. High cognitive load in the elderly, for example, can affect their center of balance (Andersson, Hagman, Talianzadeh, Svedberg, & Larsen, 2002). With increased distractions and cell phone use rising, students commonly experience high cognitive load. This increase reduces the students' academic success (Frein, Jones, & Gerow, 2013). These differences indicate the need for establishing a baseline cognitive load reaction level and comparing differences with a within-subjects design. One may draw further conclusions about task-independent complexity measurements by observing within-subject trends. Determining temporal dependencies for the cognitive load measures, on the other hand, will require nonlinear time series data analysis to uncover.

The goal is to maintain a desired difficulty level. A little stress is good for performance and leads to increased results. As difficulty increases, stress increases; if too much stress accumulates, participant performance will sharply decrease, resulting in failure for all subsequent tasks. Cognitive load through response time (RT) manipulation assessment uses many possible IV structures. This includes compound sub-task, increasing the stimulus novelty, or using a stimulus onset asynchrony (SOA).

**Dual task**

Using compound sub-tasks involves increasing intrinsic cognitive load, and subsequently RT, by adding multiple smaller tasks for the participant to follow. As there is no cognitive load offloading to germane type task, this method fails to meet the standards required for haptic–visual dual sensory input studies; too many tertiary aspects would be involved. This issue leaves us two main options for generating our cognitive load: increase novelty and unpredictability, or increase speed

**Increase novelty/unpredictability.**

Increasing the stimulus novelty or unpredictability is another option that could affect RT in this task type. Researchers often use this method when involving biological features making stimulus novelty or unpredictability a prime candidate for haptic–visual interaction studies. The issue with this IV is that it has causality limitations on human participants. This limitation makes this option for stimulus modification a poor choice, leaving one last option for us to observe.

**SOA**

A SOA is a time-pressure alteration technique that designates the amount of time between the start of one stimulus and the start of another stimulus. In studies that use two stimuli, a prime, and a target, researchers need a method to measure from the beginning of the prime until the beginning of the target. This rapid stimuli progression timer, the SOA, can be manipulated to determine effects on other dependent measures such as response time or brain activity (Harley, 2013). This metric is the measurement commonly used in multi-sensory studies due to the rapid natural interaction observed. The inspiration for the current study includes this measurement type using a mask for the second stimulus that rapidly covers up the prime (Festman, Adam, Pratt, & Fischer, 2013). The

commonly cited issue with this data type is that priming effects differ depending on priming stimulus length, causing equivalency issues in differing IV lengths (Spruyt, Hermans, Houwer, & Eelen, 2003). To overcome this issue in the present study, one can use the mask as an information block rather than inducing a prime with the first stimulus. Effectively, this modification creates a single stimulus SOA that can be temporally manipulated and therefore nullifies the issue.

### **Performance indicators of task difficulty**

#### **Response time**

The idea behind RT is simple: the more mentally involved a problem is, the longer it takes to process (Donders, 1969; Sternberg, 1969). If one devises a mental task that differs only in that it requires an extra mental process, one could determine the difference using RT; researchers call this process “Mental Chronometry” (Posner, 2005). RT has been used to observe many phenomena throughout psychology’s history, and often RT changes indicate systemic interactions. The cognitive load index creation allowed many cognitive load measurements to be standardized and analyzed using linear statistical fashions, such as one-way analysis of variance (ANOVA) and logistic regressions (Paas, Van Merriënboer, & Jeroen, 1993). More recent RT task modifications include the implicit-association task (IAT) (Greenwald, McGhee, & Schwartz, 1998), lie detection (Walczyk, Igou, Dixon, & Tcholakian, 2013), and even stress discrimination (Setz, et al., 2010). When applied to system interactions, the different variables are the systems in question, and any increase in RT would show that there was an interaction.

### **Accuracy**

A hit is a correct answer to a question about the stimulus (e.g. did a letter appear?); a miss is an incorrect answer to the same question type. One way to use this information is in the form of  $d'$ , a simple relationship of hits to false alarms. The problem is that  $d'$  is a dimensionless task-dependent statistic; a higher value simply indicates that the signal is easier to detect (Macmillan, 2002). Speed and accuracy are the general variables of interest and are measured in the RT and error rate format. There is a trade-off, known as the speed-accuracy trade-off (SAT), between these variables. The SAT has a neurological basis showing saccadic response tasks activate the superior colliculus and the lateral intraparietal area (LIP), and motor response tasks activate the primary motor cortex rather than the associated sensory areas (Bogacz, Wagenmakers, Forstmann, & Nieuwenhuis, 2010). This revelation on SAT origins makes haptic-visual dual sensory input a prime location for study on embodiment theories (Ashenfelter, Boker, Waddell, & Vitanov, 2009). One could also see implications for systems theory, provided the DV involved activates the primary motor cortex and the occipital lobe simultaneously making nonlinear analysis an ideal analytical method.

### **Limitations**

The choices for analyzing performance data are often problematic. Observations in power law show that performance is not a linear process (Bak, 1996). Any linear measure performed on a nonlinear process will be task-dependant and only show a temporarily-void representation of the specific data point separated from the system's entirety (Douc, Moulines, & Stoffer, 2014). The general options, standard summary statistics, OLS/GLM, and ANOVA fall into this category and fail to account for the extraneous var-

ables due to their rigidity. To better account for these variables one can work with the nonlinear nature involved and model the system as it transpires in time (Abraham, Abraham, & Shaw, 1990).

### **An alternative**

A measure that has already been found to be task-independent is complexity (Robinson, 2001). The ability to extract this measure from a time series would create a way to bypass current dependency on linear task-dependent measurements. \*\*Both speed and accuracy are a coupled system (Wickelgren, 1977); if one desires a task independent measure for cognitive load, one would need to look for another difficulty measure. Extracting this dimension from a time series would create a way to bypass current dependency on linear task-dependent measurements.

### **Time Series Analyses**

Time series are different from static data; for example, they violate the independent samples assumption (Shumway & Stoffer, 2011; Douc, Moulines, & Stoffer, 2014). In studies where participants contribute only a single data point (perhaps a mean) to a collective data set, the system/participant resets to time zero between runs. This reset does not happen when participants contribute multiple data points across time; performance is related to performance at previous times and to future performance. This relationship between past and future is known as an autocorrelation. Time series analysis proceeds from a plot of the raw data that reveals maxima, minima, central tendency, trends, clustering, or other features indicative of anomalies or structural issues that need resolution before proceeding. This analysis type is a three-step process. The first step is a pre-whitening process that involves removing autocorrelations and smoothing the time series.

The second step is decomposition, which involves using various techniques to extract data from the time series. Finally, the third step is analysis where one makes meaning of the presented information.

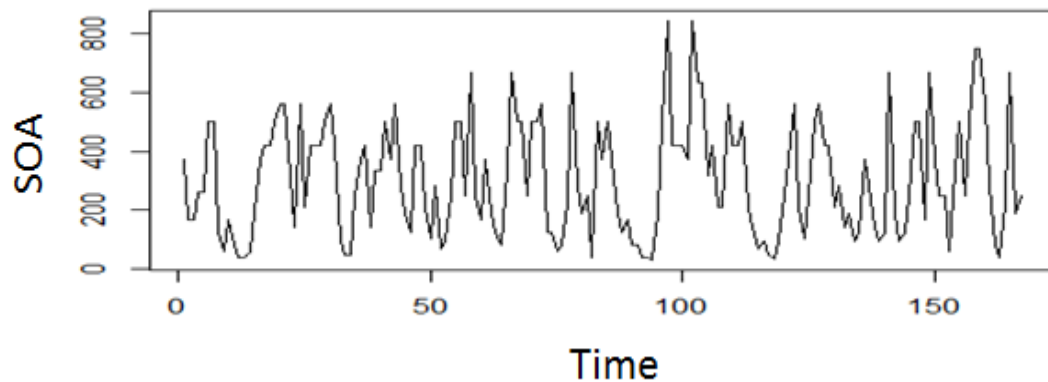


*Figure 1.* One time series created from participant 1 block 1.

### **Pre-whitening.**

When analyzing a time series the first thing one should do is observe the raw data plotted out. From this plot (Figure 1), one can quickly decipher the maximum, minimum, and possibly mean data points; it is also possible to see overarching trends, data clustering, anomalies, linearity, and structural issues among other factors. After looking at those descriptive details, one needs to recognize that a time series has a vast number of differences from normal statistical data. By far the largest difference is the independent sample assumption violation; all samples relate to the previous trial, creating autocorrelations that have to be removed. Dealing with autocorrelations is one of the first tasks performed. The most common way one accomplishes this task is by using an autoregressive algorithm that delineates the data, then rotates the data to allow for a mean with no slope, and standardizes it around a zero mean, much like z-scores (Figure 2). In our sample

(Figure 1) the data has very little linear slope to it so we do not need to delineate, but note that after we remove autocorrelations (Figure 2), the data is now set around a mean of 0. The output for this section still has large spikes and trends that one needs to account for in the next process.

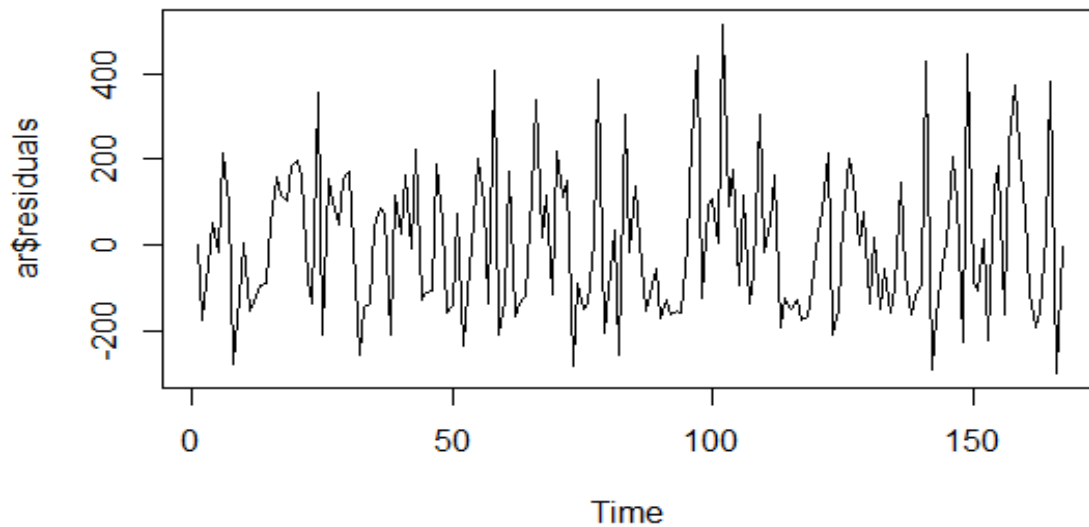


*Figure 2.* An ARIMA procedure is applied to figure 1 to remove autocorrelations.

### **Smoothing.**

The next section in the pre-whitening process is to select and apply a smoothing algorithm (Shumway & Stoffer, 2011). The most common process employed here is a moving average algorithm. In this process, one averages the first  $n_i$  (example slots [1,2] on Figure 3) numbers from a data set together. Then one averages  $n_{i+1}$  (example slots [2,3] on Figure 3). This process continues until the end of the data set. One then drops any final remaining numbers. One can use any set size he/she wants with this process; the larger the set the smoother the time series will be. It is important to note that using



sets that are too large for the time series will erase sessional trends from the data, making it linear in nature.

Original Numbers	Moving Average
24	
13	18.5
10	11.5
21	15.5
6	13.5
18	12
13	

*Figure 3: A moving average algorithm applied to a random number set.*

The output from the pre-whitening processes is smoothed and standardized, making it ready for decomposition. The most common model for this process is the Auto-Regressive Integrated Moving Averages model (ARIMA)<sup>Eq1</sup>. This portion is an art form that relies on knowledge of one's data to know the proper correction level. Although standardizing the data is a safe process, over smoothing a time series can radically alter or even destroy one's data. Although it is academically accepted, the smoothing process is frowned upon in several statistics circles, and mostly unnecessary in our situation. For this reason, minimal smoothing technique usage will be performed in this study. One should also note that wavelet transforms are the derivative of a smoothing function; the larger the scale, the smoother the time series will be, further reducing our need to smooth the time series as one already accounts for roughness in the system (Sun & Tang, 2002).

---

<sup>Eq1</sup>  $(1 - \sum_{i=1}^p \phi_i L^i) 1 - L^d X_t = \delta + (1 + \sum_{i=1}^q \theta_i L^i) \varepsilon_t$

This transformation allows us to remove the noise from the signal using thresholding techniques instead of moving averages.

### Representation

The scale at which a system is measured directly influences how coupled location and velocity are to each other (Abraham & Shaw, 1992). Scale in the present scenario is how close one looks at a signal, and velocity equates to temporal accountability. The smaller the scale we use, the less temporal accountability we will have. The way around this issue is to use probabilistic terms and measure using multiple wave frequencies at multiple locations.

One common method employed to work around this coupling issue is the Fourier transform ( $\mathcal{F}$ ) (Bracewell, 1986; Strang, 1993). If one is mapping a function in  $\mathbb{R}$ , the formula takes the equation<sup>Eq3</sup>, forcing one to “freeze” the signal at temporal location  $f(\chi)$ . If one desires variables to be located temporally, an inverse function is used<sup>Eq4</sup>. This freezing allows one to focus in on either spatial or temporal signal aspects by sacrificing the ability to view the other. Using  $\mathcal{F}$  is useful for mapping functions requiring time-frequency relationships so long as one is not attempting to localize the signal. This transform has some associated issues. The first issue is that  $\mathcal{F}$  assumes signals are infinite series segments; this assumption may be at odds with most biological systems as they are created or destroyed at intervals and do not last forever. The second issue is the inability for  $\mathcal{F}$  to localize changes; any interaction with the signal will cause effects over the signal’s entirety. In order to achieve a simultaneous time and frequency representation, one needs to use a continuous wavelet transform (CWT).

---


$$\begin{aligned} \text{Eq3 } \hat{f}(\xi) &= \int_{-\infty}^{\infty} f(\chi) e^{-2i\chi\xi} d\chi \\ \text{Eq4 } f(\chi) &= \int_{-\infty}^{\infty} \hat{f}(\xi) e^{2i\xi\chi} d\xi \end{aligned}$$

**Decomposition (Why not Fourier).**

In the second phase, time series decomposition techniques are employed. This step involves selecting how one wants to represent the signal. Depending on choices such as regression analysis, Fourier analyses, wavelet analysis, or the many other methods the end-result from the processing will be drastically different.

Performing regression analysis requires minimal alteration to the series. In effect, this is the result of over-smoothing until all that is left is the mean (Shumway & Stoffer, 2011). Although this method will display trends and allow for prediction models, it is often the least effective analytical method as it fails to account for sessional trends and frequency domain alterations. Researchers usually perform regression analysis on the time domain in a time series.

A Fourier analysis is the classic signal analysis tool. This tool can be used to display the time domain or the frequency domain and requires little alteration to the signal (Shumway & Stoffer, 2011). Its inability to display both the time and frequency domain and the inability to localize changes in the system can be crippling for many researchers. One attempt to circumvent this crippling effect is to cut the time series into segments, but this process raises another issue. If one wishes to perform analyses on a signal thousands of cases long, and needs fine grain detail, he/she will have to break the signal into hundreds of segments. When there are alternative methods, it becomes difficult to justify this analysis.

The preferred method of choice by researchers when needing simultaneous time and frequency domain analysis with fine grain detail is wavelet analysis (Douc, Moulines, & Stoffer, 2014). Although it requires drastic alterations to the signal representation, it is

unparalleled in its ability to localize changes in both domains and provides easy-to-read output.

### **Wavelet Transform Modulus Maxima**

Wavelet Transform Modulus Maxima (WTMM) is a means to represent the fine-grain structure of signals (Walker, 2008). The WTMM method uses continuous wavelet transform rather than Fourier transforms to detect singularities, otherwise known as discontinuities or areas in the signal that are not continuous at a particular location. WTMM is useful when for signals with multiple fractal dimensions or when simultaneous time and frequency domain detail is desirable (Douc, Moulines, & Stoffer, 2014). WTMM, often referred to as a "mathematical microscope," is able to display multiple simultaneous scales making it easier to sort signal information out from noise, sections of the time series that may be extraneous or chaotic.

### **Wavelets and scales (windows).**

When performing this analysis type one first needs to select a mother wavelet. The mother wavelet is the ruler by which all rulers in this type of analysis exist and is the unmodified version of the daughter wavelets used in the next section. Each wavelet type has a different sensitivity level making the choice an important one that depends on the signal at which one is looking (Walker, 2008; Douc, Moulines, & Stoffer, 2014). In terms of choosing the mother wavelet, a wavelet's usefulness is normally determined by its numbers of vanishing moments (Sun & Tang, 2002). A vanishing moment is determined by the number of polynomials required in the equation to create it (Mallat, 2009). A wavelet with two vanishing moments is ideal for processing velocity signals. In the current study, as the study is using a time series based on hand movements to detect ob-

ject recognition speed and accuracy, one would use the Gaussian second derivative (Mexican Hat<sup>Eq11</sup>) wavelet (Figure 4) which has two vanishing moments.

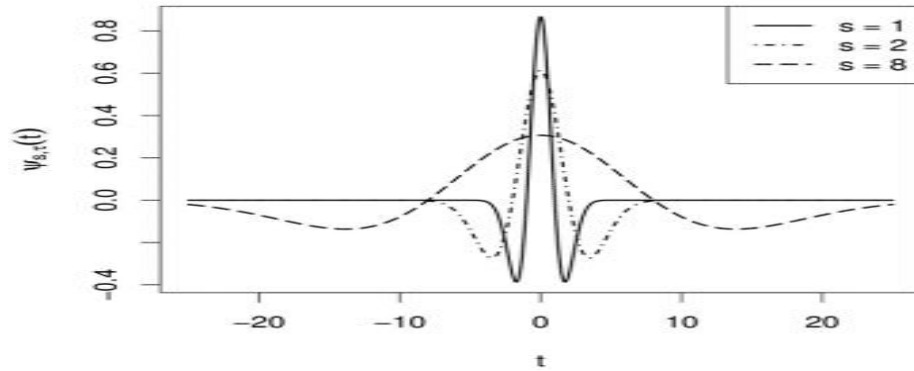


Figure 4. A gaussian2 wavelet shown at multiple scale variations.

### Iterations and correlations.

The next step in the wavelet transform modulus maxima (WTMM) method was to use a continuous wavelet transform (CWT) to convert the data into a graph. This conversion process involves applying the wavelet to the time series at differing periods and taking the correlation coefficients for that scale (a) and location (b) and creating a correlation matrix from the corresponding values (Figure 5). One can then assign these values colors and plot them as a heat-map (Figure 6).

---


$$\text{Eq11} (t) = \frac{2}{\sqrt{3\sigma\pi^4}} \left(1 - \frac{t^2}{\sigma^2}\right) e^{-\frac{t^2}{2\sigma^2}}$$

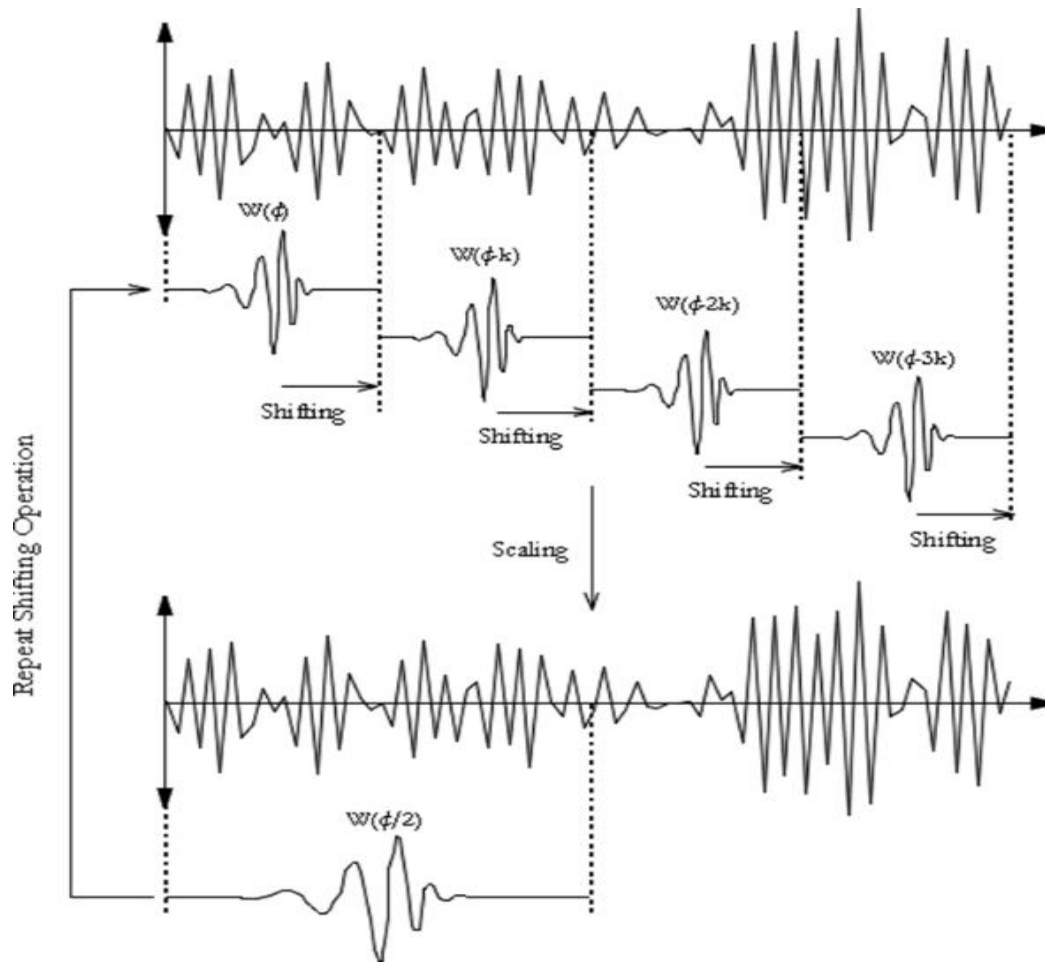
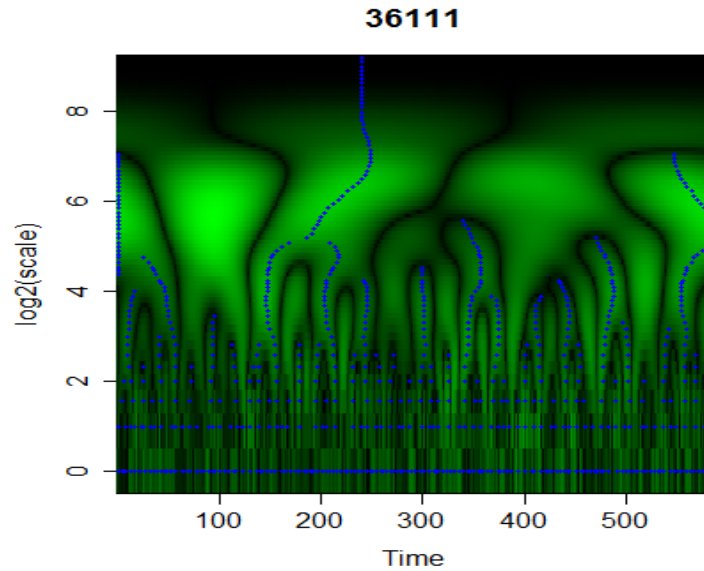


Figure 5: Wavelet being applied to a time series in the CWT process.

One can then use this heat-map to expose fractal properties visually and create the signal's graphic profile. The x-axis displays the fractal's temporal aspects, allowing us to track changes in the converted TMU sequence. The y-axis the scale is displayed showing recursion over time and outlining nested systems. The dark lines prevalent in the figure show zero-correlation areas, known as separatrices, dividing the system state-space and outlining any bifurcations as the system descends into chaos. One should note that this chaos is not random or uncontrolled fluctuation in the system, but it is a resolution factor and our current perceptual and technological limitations.



*Figure 6:* Outlining the contour lines of a CWT in order to create the WTMM tree structure.

### **Maxima and Singularities.**

In order to gain a more clear view, one needs to outline the maxima in the CWT image and abstract them to create a WTMM tree structure (Figure 7). One property observed in local singularities is that they suffer from exponential decay in the WTMM tree structure. Maxima ridges caused by noise, especially white noise, do not proliferate to large scales (Mallat & Hwang, 1992). More simply stated, the higher the scale that a branch reaches, the less likely that it is due to noise allowing us to observe a visual version of a p-value. This also means that on its own WTMM is not appropriate for ultra-high frequency signals, as they will also display as noise (Sun & Tang, 2002). There are ways to overcome these phenomena, but they are not necessary at present. Using thresholding techniques, one is able to isolate the probable signal branches from the noise and create a basic outline using the maxima peaks. Using these peaks to regenerate the signal one is able to localize changes in the signal without affecting the system's entirety.

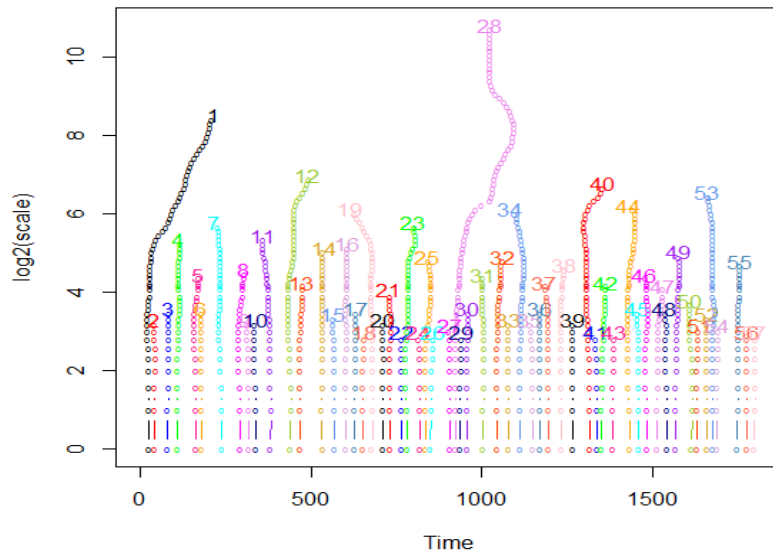


Figure 7: Maxima contour lines abstracted from the CWT plot.

### Measuring the System

Isolating the signal from the noise using WTMM is only part of the process; there are multiple measurements worth extracting from the remaining signal and multiple ways to extract them. Unlike linear measurements such as  $d'$ , these measures are often multi-dimensional; meaning the way they are represented determines their use. The more common measurements—Hurst exponents, Holder exponents, and Fractal Dimension—each reveal different aspects of the signal.

**Hurst exponent.** The Hurst exponent ( $H$ ), also referred to as the "index of long-range dependence," quantifies a time series tendency to regress to the mean or to cluster in a particular direction (Kleinow, 2002). A value in the range 0.5–1 indicates a time series with positive long-term autocorrelations, meaning a high value in the series will follow other high values and will rise with time. A value in the range 0 – 0.5 indicates long-term switching between high and low values in a time series; single high values will like-



ly be followed by low, with this tendency lasting a long time into the future. A value of  $H=0.5$  indicates a completely uncorrelated series. As one already removed autocorrelations, this value should remain fairly close to  $H=0.5$ , but local estimates of Hurst values can be determined using the formula  $H = 2 - (f_{(\alpha)})$ . This value is a local Hurst and not a guarantee of long-term dependencies.

**The Holder exponent.** The Holder exponent ( $\alpha$ ), also known as the “singularity exponent,” quantifies the level of roughness in a system (Mallat, 2009). On the Holder spectrum, a rougher state-space is chaotic, a smooth state-space is orderly, and everything exists in the gradients in between. The median  $\alpha$  depends on how the measurements in the spectrum are standardized. Often, as is the case in this paper, zero is the line on the graph that divides chaos on the negative side and order on the positive side. The higher the  $\alpha$  value, the more orderly the system is and the lower the value the more chaotic it is. Another important factor about  $\alpha$  is the range between  $\alpha_{(max)}$  and  $\alpha_{(min)}$ . The larger the range, the more sensitive the system is to fluctuations.

**Fractal Dimension.** Mathematically a dimension is the number of points required to represent a system. A single point is zero dimensions, a line is one, and a plane is two. In systems, this dimensionality works the same way with one exception. The closer one looks at a system, the more numerous interdependent systems one will see. How close one looks is referred to as the scale. How these differing scales relate to each other is the fractal dimension. This measurement is used to assess system complexity (Mandelbrot, 1983). If one looks at any independent system part, one will likely find base biological functions that allow proper performance. Investigation into how these parts work may

allow us to reassemble a model that more accurately represents the way guidance works in a dynamical way, removing some unnecessary compartmentalization in the process.

**Multifractal spectra.** By tracking how often a specific  $\alpha$  value appears, one can determine the fractal dimensionality of a system using the continuous function  $f_{(\alpha)}$  as it is related by a Legendre transformation (Halsey, Jensen, Kadanoff, Procaccia, & Shraiman, 1986; Lyra & Tsallis, 1998). The easiest way to do this is by using a multifractal spectrum. In the multifractal spectrum, one is graphing  $\alpha$  on the x-axis to determine  $f_{(\alpha)}$  on the y-axis. By displaying the values like this, one can quickly see several data features. The maximum  $f_{(\alpha)}$  value is also the Hausdorff Dimension  $D_{(box)}$  making it another complexity measurement. Viewing  $D_{(Box)}$  as the non-negative real number associated with any metric space, one can further generalize the notion of the dimension of a real vector space. For example,  $D_{(Box)}$  of a point is zero, a line is one, and a plane is two. One can also observe the location  $\alpha_{min}$  and  $\alpha_{max}$ ; these locations are also known as  $D_{\infty}$  and  $D_{-\infty}$  and are respectively where measurements are most concentrated and most rarefied. Observing the graph shape and consistency as a whole allows for quick complexity and stability assessments in the system. The narrower the spectrum is  $D_{\infty} - D_{-\infty}$  the less sensitive it is to temporal scales. The closer this number gets to zero the more likely it is to be mono-fractal in nature. Using this layout it is also possible to determine the entropy index (q), a measure of uncertainty contained in the system<sup>Eq12</sup> (Lyra & Tsallis, 1998). As task complexity further equates to cognitive load, one can make task-independent visual assessment of the cognitive load involved in a system.

---


$$\text{Eq12 } \frac{1}{1-q} = \frac{1}{\alpha_{(max)}} - \frac{1}{\alpha_{(min)}}$$

**Self-organization of performance (predictions)**

In the current context, the antecedent to chaos is order and this correlates on the multifractal spectrum as positive or negative values on the x-axis ( $\alpha$ ). One can think of order and chaos as the amount of rules the system follows. Some rules are required to predict the system, but too many rules and nothing interesting will ever happen. Chaos is simply the flexibility within the rules. A self-organizing system naturally trends to chaos or order like every other system, but after straying too far from its balance it will correct itself by altering the rules. This process should present itself in a natural pull towards neutrality on the multifractal spectrum ( $\alpha=0$ ) that coincides with a change in speed or accuracy.

**Replication of near-hand effect.** Festman et al (2013) showed that there are stimulus detection performance benefits from nearness-to-hand. By replicating these benefits, we have a mechanism to test our cognitive load measurements against and a tool to show the efficiency using complexity measures can provide. Specific measurements are useful for specific situations, but sometimes one needs to know general rules for general measures. Task-independent measurements are more generalizable and applicable to situations that may otherwise be untestable.

**More subtle effects (potential to see SOC).** Orderliness in the signal appears as positive or negative  $\alpha$  values in the multifractal spectrum. This orderliness allows the potential to observe self-organized critical aspects that can be used to create many other task-independent measurements. These effects would be undetectable with linear techniques (Douc, Moulines, & Stoffer, 2014; Mallat, 2009). As complexity is a non-linear

measure, its multidimensionality may be useful in teasing out other non-apparent fine-grain data features. Revealing self-organized critical systems allows for better modeling techniques and more natural views of cognition. One can use these features to make a pseudo-predictive long-term forecast by indicating that our visual system exhibits power-law-like behaviors. Further assessment of task-independencies involves Chinese participant observing Chinese stimuli to be included. As the two languages and cultures are drastically different, normal descriptive measures should differ slightly, while task-independent measures should remain relatively the same. This postulated difference allows for investigation into whether or not complexity is task-independent as claimed or if it is inadequate.

## **Method**

### **Participants**

Ten right-handed, university students (five native English speakers and five native Chinese speakers, each with normal or corrected vision) volunteered for individual 30-minute sessions over 4 weeks. (Including two native languages reduced the potential for artefacts of alphabet choice.) Each session was separated by at least one hour to reduce potential fatigue effects and the first 40 trials of each session were devoted to practicing the *mouse-manipulation-plus-target-identification* coordination task before data collection; each participant contributed about 1440–1920 trials in total.

### **Materials**

Each participant stood upright before a platform that constituted the top level of a two-level, customized computer desk. Above the platform, held by an articulating swing arm, was a 22-inch monitor (1366 x 768 pixel resolution, 65 x 41° usable viewing field,

centered at  $30^\circ$  above the horizon) connected to Dell OptiPlex 780 [2.9GHz Core2 Duo processor 4GB Ram Windows Vista 32-bit]. To the left was standard keyboard that was in view and accessible to the participant's left hand. On the bottom level, under the monitor/keyboard platform and thus out of view, was a Logitech MX510 wireless optical mouse with its software acceleration disabled and its speed adjusted such that the mouse-speed to hand-speed ratio was 1:1. Bumpers at the sides of this desktop kept the participant's right hand inside a span of about 50 cm of longitudinal movement. A 1200 Hz tone was the auditory signal to slide the mouse smoothly from the left side of the desktop to the right.

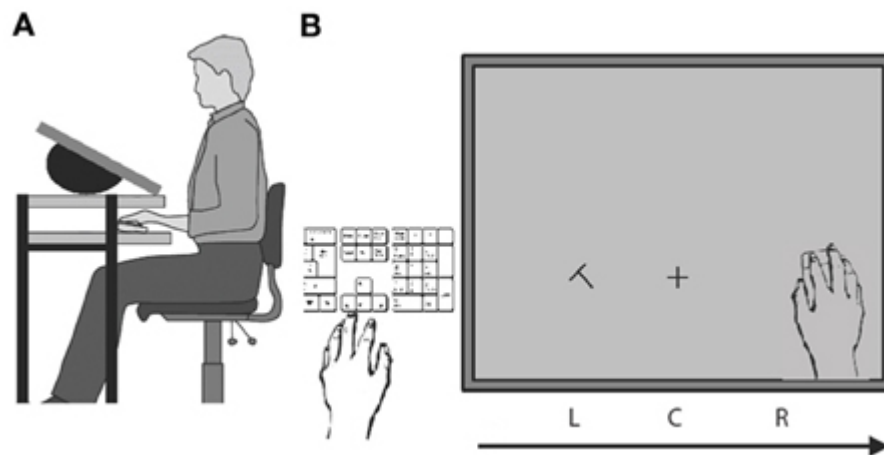


*Figure 8:* Schematic illustration of the experimental setup. (A) Side view. (B) Bird's eye view of the hands and their respective tasks. The right hand moved continuously from left to right and back again on a desktop under the display. Image adapted from Festman et al (2013).

Each trial began with a fixation point, a left-to-right centered reticle (sized  $2 \times 2^\circ$ ) in continuous view at  $6^\circ$  below midpoint. The reticle's appearance coincided with a 1200 Hz tone that signaled the beginning of the trial. Stimulus presentation was controlled by custom Python code that rendered the stimuli off-screen before display (pre-cache) for display speeds near monitor refresh rate. The target stimuli (rotated characters **T** or **L** for English speakers and 丩 and ++ for Chinese speakers) were sized  $2.4 \times 2.4^\circ$ . They ap-

peared on the left or right bottom corners of the screen while the right hand was at one of six possible mouse trajectory points during the trial. The visual stimulus remained for the length of the SOA at that mouse location before being occluded by a square black mask until the trials conclusion.

### **Procedure**

Each session included 1 block of 240 trials (two target characters x two target locations x six mouse locations x 240 repetitions) and took under 30 minutes. Each block consisted of 240 trials with probe presentation (10 trials per condition). Each trial began with resetting the mouse cursor to the left screen location and a 1200 Hz tone that signaled the participant to slide the mouse smoothly from the left to the right side of the desktop (about 52 cm). Thus, the mouse's trajectory crossed six critical points on the desktop: 3 left and 3 right (all equally spaced 8.6cm measurements) while moving left-to-right. Trials were separated by an instruction screen requesting keyboard input for the character displayed in the previous trial.

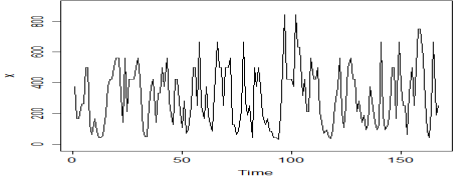
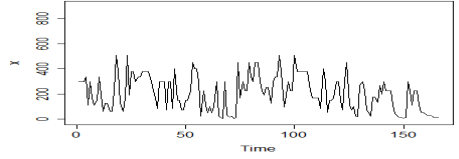
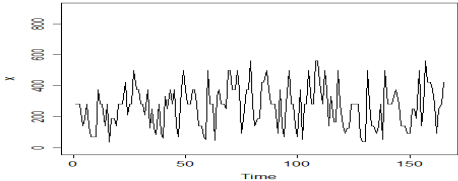
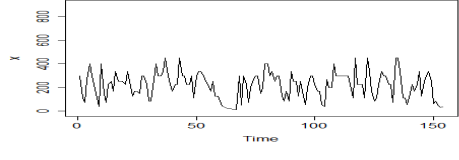
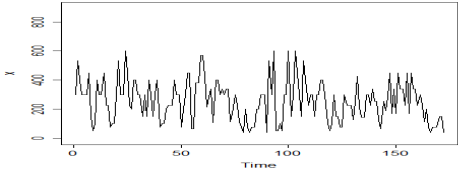
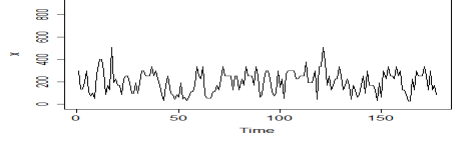
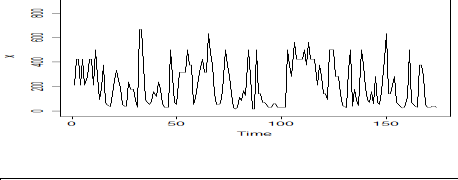
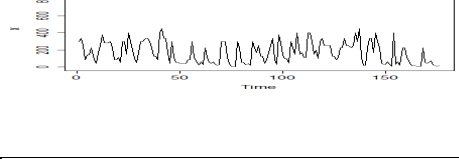
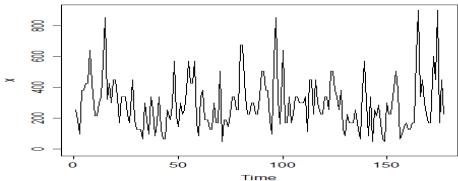
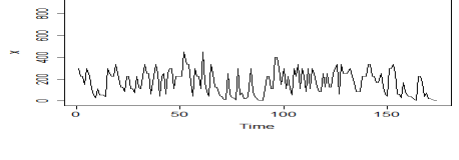
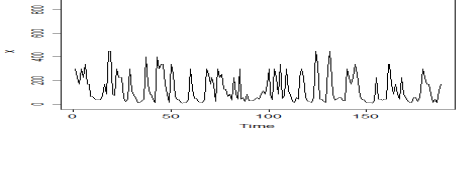
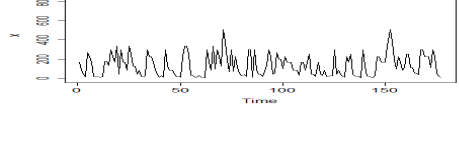
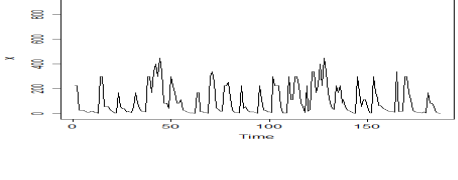
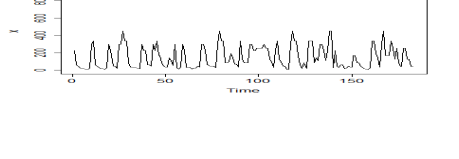
Selection of target character, target location, and mouse location were randomized across trials using a separate randomizer for each IV (character, location, and mouse location). The target appeared when the mouse was at one of the six mouse trajectory points and remained visible for the length of the SOA at that mouse location before being occluded by a square black mask until the trials conclusion whereupon the participant used her or his left hand to indicate the target's identity by pressing **T** or **L** the on the keyboard (↵ and ⇞ stickers placed over the T and L keys for Chinese characters). SOAs (the time between stimulus presentation and masking) were continuously adjusted via an adaptive staircase procedure.

The session began with a 300ms lag between the onset of stimulus presentation and stimulus masking which decreased by 25% after every two consecutive correct responses but increased by 25% after each error response such that accuracy remained at the 70% average detection rate (between 65% and 75% accuracy overall). This difference is about 10% tighter than Festman et al. due to SOAs being computer adjusted instead of manually. The first 40 trials provided sufficient practice that SOAs were reduced to <225ms on average, too short an interval for most participants to produce a stable eye fixation. SOAs were continuously recorded and adjusted by the computer after each response and used as the inputs to the WTMM procedure.

### Data Analysis

**Separation into blocks.** To best view these system types one desired as little original data modification as possible. The data are sorted as follows; all SOA's attached to incorrect responses were discarded. Each participant block was sorted according to presentation order. Using hand location as a temporal measurement, one can create a time unit 6 measurements in length that one can use as a temporal measurement unit (TMU). One can then specify multiple TMUs using the stimulus location, creating a strophic plane system view (Abraham & Shaw, 1992) that gives one the completed time series (Table 1). To allow for more divergence between blocks and save space the first and last blocks were included in the description, and further information is provided using an internet link (see Appendix A).

Participant	Beginning	End
English Participants		

Participant 1		
Participant 2		
Participant 3		
Participant 4		
Participant 5		
Chinese Participants		
Participant 6		
Participant 7		



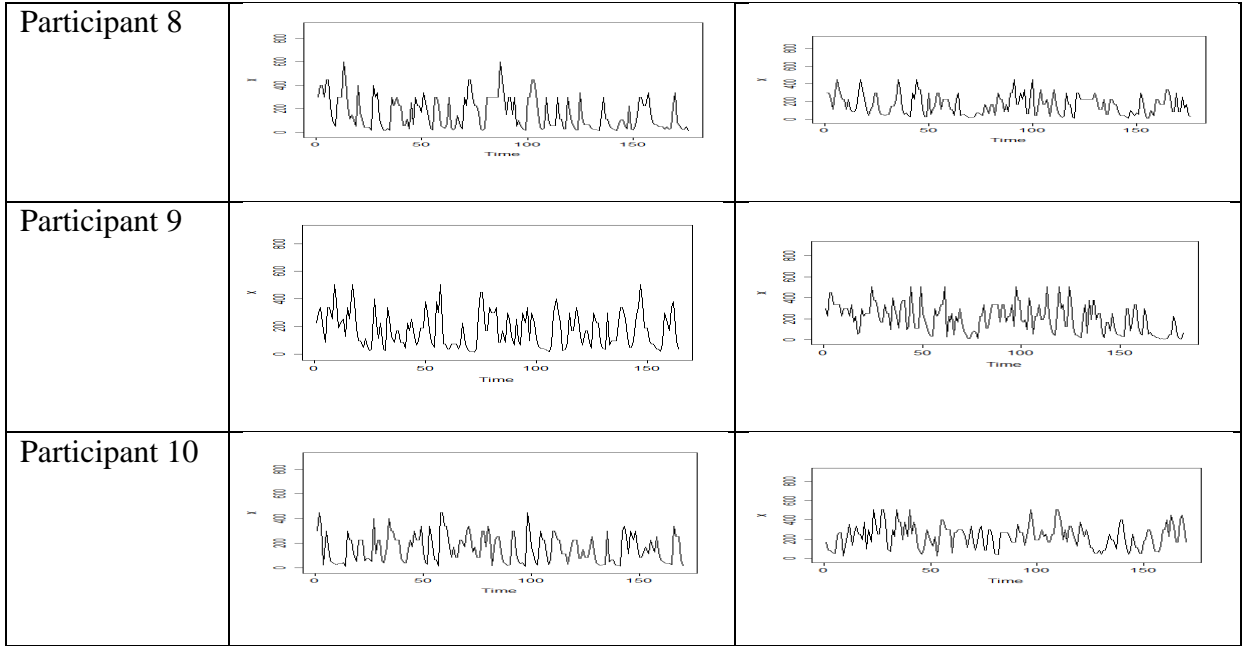
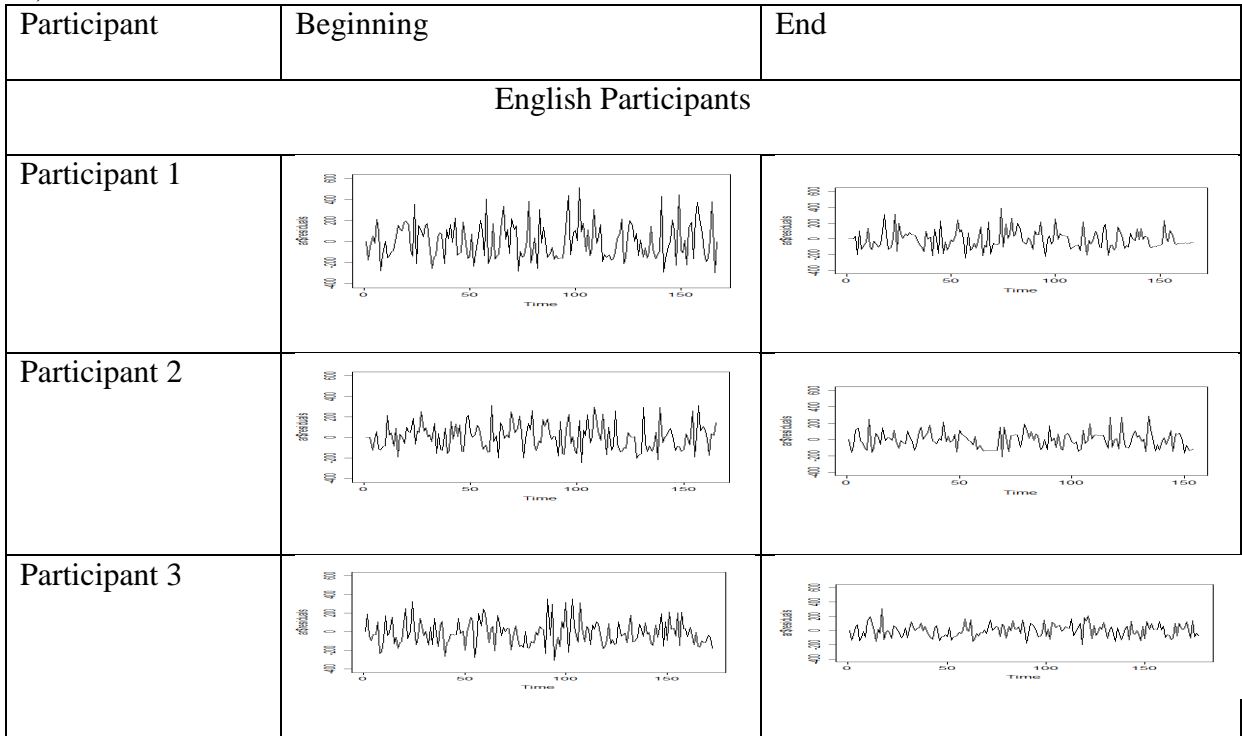


Table 1: The raw time series for each participant’s first and last block, SOA<sub>(x-axis max=900)</sub> and Time<sub>(y-axis max=200)</sub>.

**Pre-whitening.** After creating a time series an Auto-Regressive Integrated Moving Average (ARIMA (0,1,3)) algorithm was used to remove any autocorrelations (Table 2).



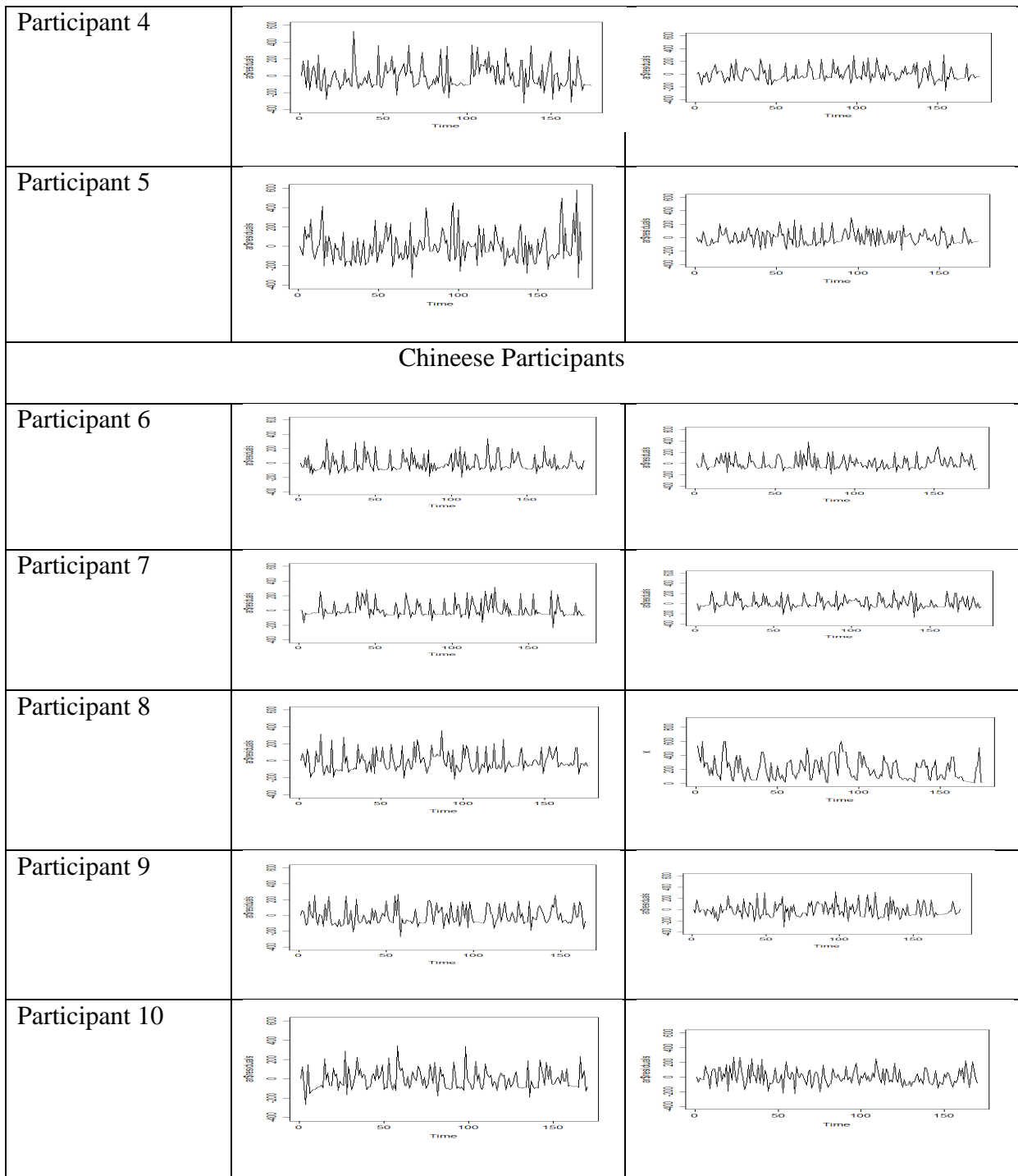


Table 2: The pre-whitened time series for each participant's first and last block SOA (x-axis max=600, min=-400) and Time (y-axis max=200).

**Decomposition into wavelets.** The mother wavelet chosen for this process is the second derivative of the Gaussian wavelet, otherwise known as the Mexican Hat wavelet.

**Iterations and correlations.** This transform was performed using R and the waveCWT package. This created a unique CWT for each block that each participant ran (Appendix A).

**Maxima and singularities.** Outlining the maxima and extracting singularities created a unique WTMM profile for each block that each participant ran (Appendix A).

**Holder exponents.** After extracting the Holder exponents, a graph with  $\alpha$  on the x-axis to determine  $f(\alpha)$  on the y-axis, the multifractal spectrum, was created for each block each participant. This information was then use for analysis.

## Results

### Near hand effect

A significant hand position effect was found when the data was split into separate one-way repeated measures ANOVA's for the each stimulus location (left and right display side) on mean performance in stimulus discrimination, with hand position (six levels) as within-subjects variable. When the probe is on the left screen side a significant effect was observed  $F(5, 60) = 3.09, p = .015, \eta^2_{partial} = .21, power = .842$ . When the probe is on the right screen side, another significant effect was observed  $F(5, 60) = 4.232, p = .002, \eta^2_{partial} = .26, power = .945$ . This finding indicates a strong preference for the hand being closer to the right screen side (Figure 9).

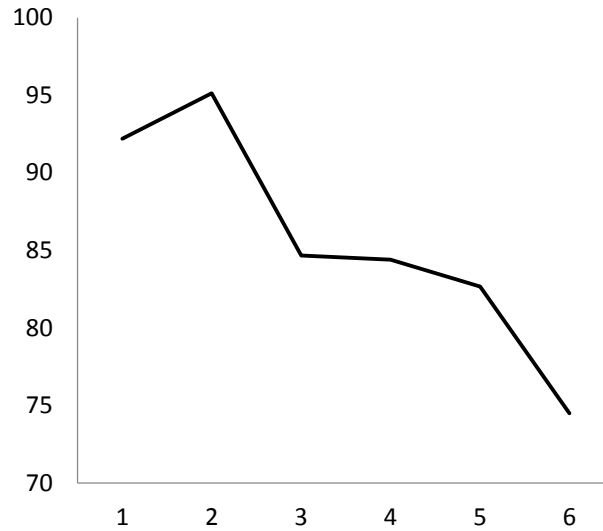


*Figure 9.* The  $\bar{x}_{(SOA)}$  in milliseconds for the total time series grouped by mouse location.

We then classified the trials according to hand proximity to the stimulus (near, medium, and far), each section correlating to approximately 7.5 inches of hand movement area, to reveal another significant effect. A two-way repeated measures ANOVA for stimulus locations (two levels) and hand proximity (three levels) as within-subjects variables using mean correct stimulus discrimination percentage as the measure was conducted revealing that hand proximity had a significant effect  $F(2, 24) = 31.74, p < .001, \eta^2_{partial} = .73, \text{power} = 1.0$ , (Figure 10). No significant preference for either stimulus presentation side was observed ( $p = .07$ ).

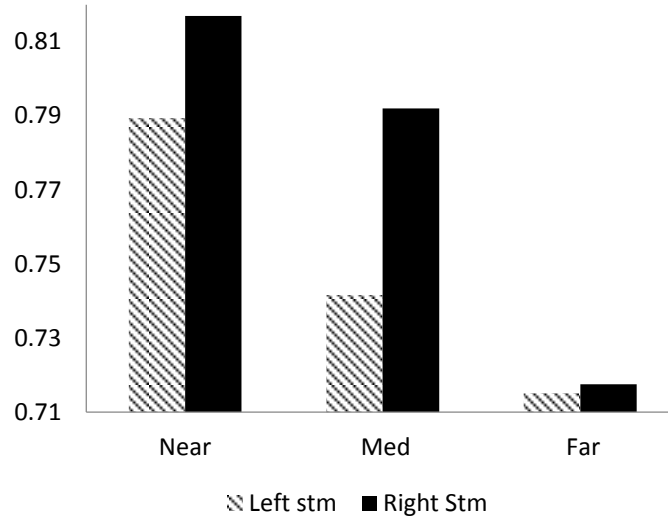


Figure 10. Mean percentage correct by hand location compared to stimulus.

**Task complexity across Ps, mean Holder exponent, and Range across each block /English and Chinese**

	English				
Block	SOA <sub>(x̄-max)</sub>	SOA <sub>(x̄-min)</sub>	Accuracy <sub>(x̄)</sub>	D <sub>(range)</sub>	D <sub>(x̄-avg)</sub>
1	0.714583333	0.026166789	71.33333333	0.746666	-0.04024
2	0.57375	0.023720703	72.83333333	0.50186	0.264002
3	0.624375	0.020009766	72.25	1.312771	-0.186902
4	0.5625	0.020853272	70.16666667	1.351442	0.173166
5	0.5015625	0.009960938	72.08333333	1.169745	-0.087008
6	0.5375	0.022338867	71.94444444	1.273203	0.101724
7	0.52734375	0.007910156	71.25	0.784629	-0.233413
8	0.478125	0.003787232	71.25	2.100837	0.045322

	Chinese				
Block	SOA <sub>(x̄-max)</sub>	SOA <sub>(x̄-min)</sub>	Accuracy <sub>(x̄)</sub>	D <sub>(range)</sub>	D <sub>(x̄-avg)</sub>
1	0.49125	0.007111416	73.75	1.275486	-0.426013
2	0.59875	0.010644531	76.16666667	1.218285	-0.075482
3	0.5175	0.006256771	75.33333333	1.536675	-0.200093
4	0.4725	0.005373611	73.75	1.210975	-0.088201
5	0.5025	0.007567063	74	1.579636	-0.218527
6	0.46875	0.006317139	74.44444444	0.810891	0.099613

	Grand Total				

Block	$SOA_{(\bar{x}\text{-max})}$	$SOA_{(\bar{x}\text{-min})}$	$Accuracy_{(\bar{x})}$	$D_{(\text{range})}$	$D_{(\bar{x}\text{-avg})}$
1	0.960208333	0.029722497	72.54166667	1.011076	-0.233126
2	0.873125	0.029042969	74.5	0.860072	0.09426
3	0.883125	0.023138151	73.79166667	1.424723	-0.193498
4	0.79875	0.023540077	71.95833333	1.281209	0.042482
5	0.7528125	0.013744469	73.04166667	1.397462	-0.160075
6	0.771875	0.025497437	73.19444444	1.042047	0.100668
7	0.52734375	0.007910156	71.25	0.784629	-0.233413
8	0.478125	0.003787232	71.25	2.100837	0.045322

Table 3: The  $\bar{x}$ - $SOA_{(\text{max})}$ ,  $\bar{x}$ - $SOA_{(\text{min})}$ ,  $\bar{x}$ -Accuracy,  $\bar{x}$ - $D_{(\text{range})}$ , and  $\bar{x}$ - $D_{(-\infty)}$  for each block (split into English, Chinese, and Total).

The WTMM output revealed that the task complexity across participants was relatively stable, fluctuating between -0.5 and .5. These findings indicate that one is observing a relatively well-developed system in all participants. In all participants,  $D_{(Box)} = 1$  indicating that at some point in every trial there was a direct line of sight between the participant and the stimulus. One can also notice that in all participants  $D_{(\infty)} < 0$  indicating the presence of chaos in all systems. As  $D_{(-\infty)}$  approaches higher positive numbers one can observe that the system is becoming more ordered. When  $D_{(-\infty)} \approx D_{(\infty)}^* - 1$  it indicates that the system is more likely to be mono-fractal. Participant 7 is the only participant to be able to score above our cutoff, indicating that the task was overly simple; this difference is reflected in the increased order found on the multifractal spectrum. Although excluded from the overall linear analysis, this participant was included in the charts to show the increased level of order that corresponded to the relative easy time the participant had with the task.

### Multifractal spectra (for each P –describe performance).

P	$SOA_{(\text{avg-max})}$	$SOA_{(\text{avg-min})}$	$Accuracy_{(\text{avg})}$	$D_{(\text{range})}$	$D_{(\text{max-avg})}$
English Participants					
1	675.000	12.625	69.600	0.584	0.225
2	506.250	24.250	67.100	0.488	0.180

3	525.000	29.700	72.750	0.595	-0.010
4	558.350	9.500	72.900	0.389	0.420
5	675.000	26.095	73.150	0.507	0.260
Total English	587.920	20.434	71.100	0.513	0.215
Chinese Participants					
6	478.150	5.300	74.400	0.647	0.115
7	450.000	0.266	77.100	0.296	0.560
8	575.000	13.000	73.300	0.413	0.350
9	506.300	10.165	72.050	0.545	0.265
10	478.150	17.750	70.800	0.567	0.055
Total Chinese	497.520	9.296	73.530	0.493	0.269
Grand Total	542.720	14.865	72.315	0.503	0.242

*Table 4:* The  $\bar{x}$ -SOA<sub>(max)</sub>,  $\bar{x}$ -SOA<sub>(min)</sub>,  $\bar{x}$ -Accuracy,  $\bar{x}$ -D<sub>(range)</sub>, and  $\bar{x}$ -D<sub>(∞)</sub> for each participant (split into English, and Chinese).

The relatively stable pattern of  $f_{(a)}$  for  $D_{(∞)}$  indicates that in all situations the participants were in a relative level of perceptual awareness. This phenomenon is likely an artifact of the experimental environment as is the overall shape. The silver ratio shape is also a reflection of the task. Essentially, it indicates that the participant's search pattern involved repeatedly cutting the screen in half until he/she acquired the target. In participants 1,2,3, and 8 one can observe both a decrease in chaos in the system  $D_{(∞)}$  and a decrease in  $\bar{x}_{(SOA)}$  in each SOA. One can also witness the system becoming more chaotic and then regressing toward the mean in the subsequent trials.

As noted earlier, participant 7 showed correct responses that were abnormal; the relative ease this participant had with the task is reflected in the  $D_{(∞)}$  at 0.83. The stable  $\bar{x}_{(SOA)}$  and accuracy across trials leads us to believe that the decrease in  $D_{(∞)}$  in the final trial may be due to the task becoming overly simplistic and the participant losing interest. Participant 6 and 9 were relatively stable across all measurements, but the spectrum reveals that the system is tightening up. Previous trials of this participant indicate that they oscillate between ordered and chaotic blocks and rapid regress toward the mean in the

following blocks. This finding, combined with the relatively high over all accuracy (both hit 75%), indicates that these participants both have well developed visual search systems that exhibit smaller over changes between blocks.

Participants 4 and 5 both show a drop in order between the first and last blocks. Once again, one notices the rapid oscillations between higher order and lower order between blocks, with the regression to the mean observed with all the others. Participant 10 remained stable over all the blocks, indicating little learning. As the accuracy was lower than the other stable participants' accuracy, she was not included in the group that found the task too simple at first. With further investigation, one can notice that the  $f_{(\alpha)}$  for this participant was tighter than the other participants  $f_{(\alpha)}$ , indicating an increased constant alertness level. In light of that finding, we decided to investigate further. By linking all the blocks together, a longer time series was created for further analysis. The resulting multifractal spectrum (Figure 11) indicated that this participant likely also found this task to be easy, demonstrated by the participant's behavior exhibiting a high overall order and little variability over the blocks.



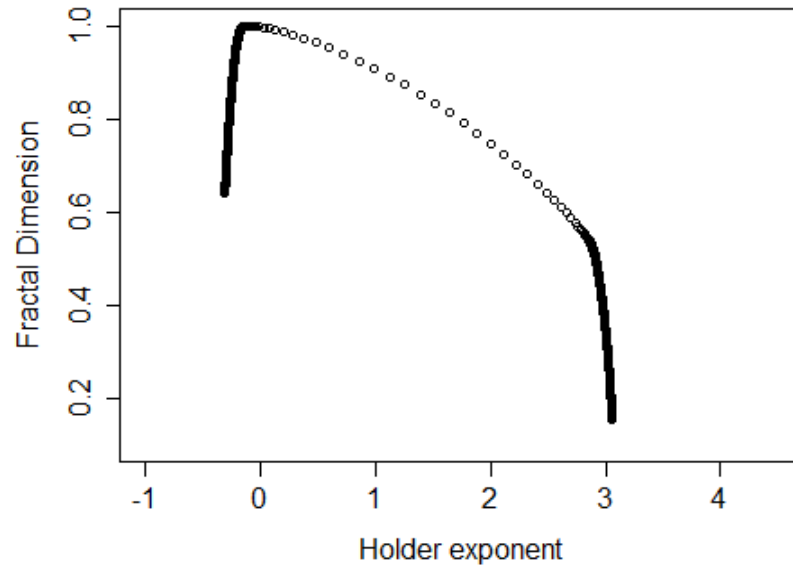


Figure 11: Multifractal spectrum for participant 10, all trials combined.

Participant	Beginning	End
Participant 1		
Participant 2		
Participant 3		

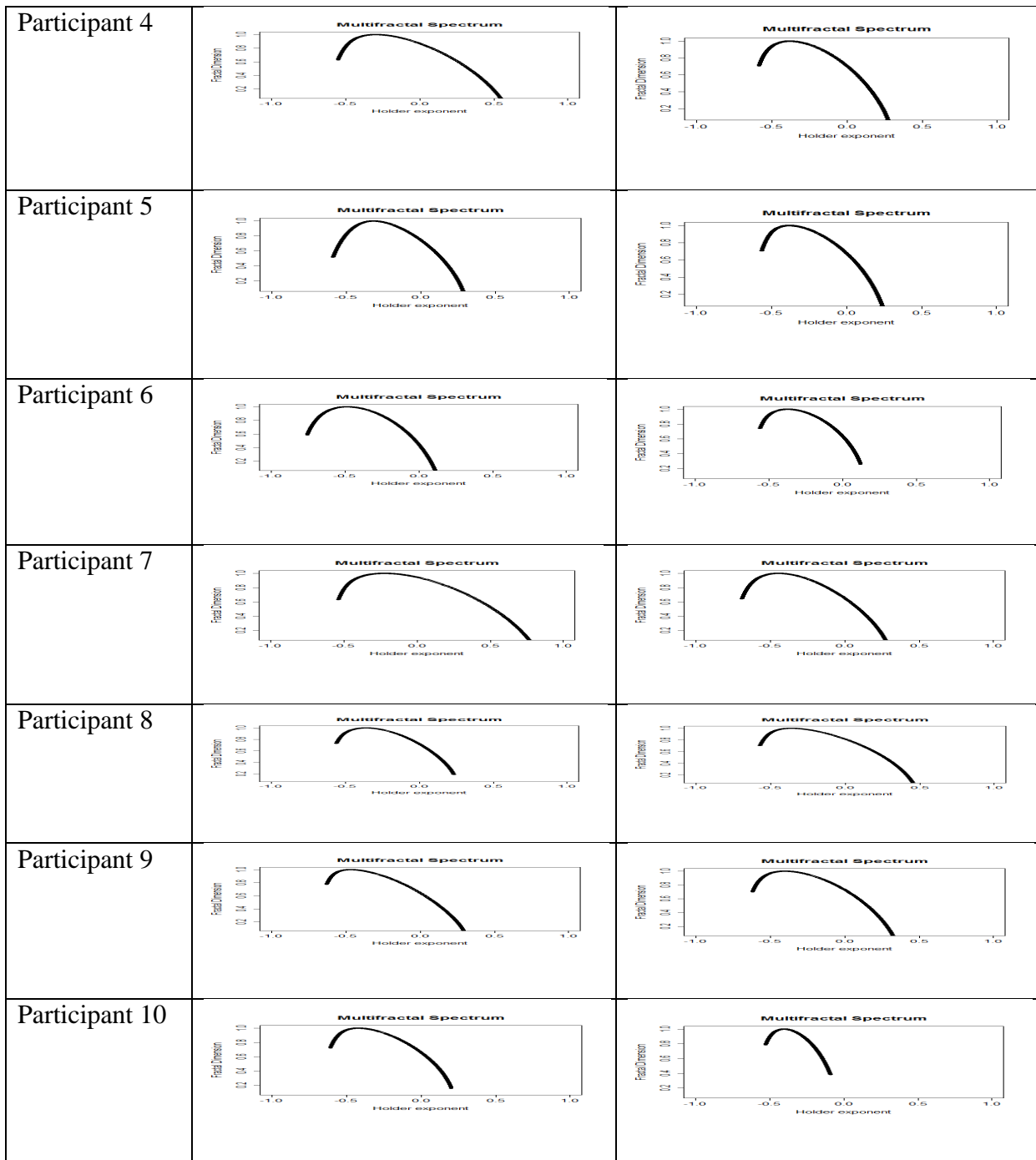


Table 5: This is the multifractal spectrum for each participant's first and last block.

## Discussion

### Replication of near-hand effect

Using the initial linear analysis, one can observe the findings, and the reduction in size due to trimming the data both closely reflected past researcher's findings. In the

graph comparisons (Figure 12), one can see that the standard error for the current study is comparable to prior findings, and our distance effects are more pronounced. As we only moved the hand one direction Graph C should be compared to the “away” data in graph A, and the “toward” data in graph B. These findings reflect a successful replication and closely correlate with the expected findings suggested by embodied cognition research.

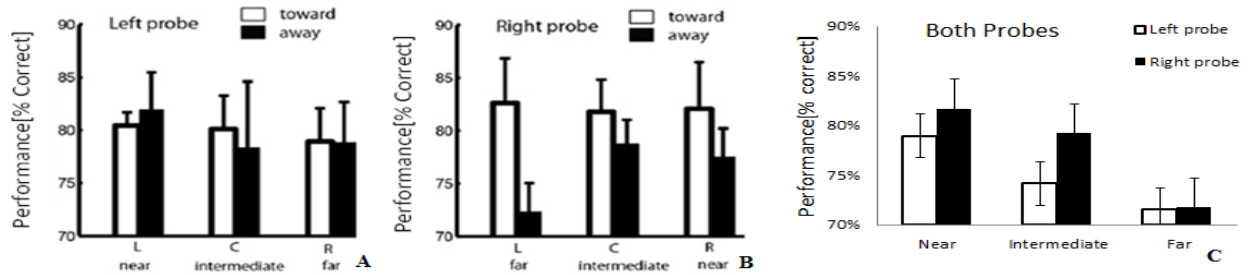


Figure 12: The results obtained in the Festman et al (2013) for comparison. Graph A and B are the Festman results, Graph C are currently obtained results. Figures A&B adapted from Festman et al (2013).

### Self-organization of performance

Overall self-organization of performance was observed around the mean Holder exponent for all participants. This finding indicates a self-correcting system that likely follows a power-law structure. With a small  $\bar{x}\text{-}D_{(\text{range})}$  ( $<1$  for all participants) the system is relatively stable over the long run. Further studies will be required to find the exact equation, but one should be able to model the system using a single solution equation.

**SOA as index of performance.** Although SOA change was an effective post-hoc indication of a catastrophic change in the system, there was little indication when that change would occur using it beforehand, as it is a task-dependent measure. Also, SOA appears to be task-dependent as both the maximum and minimum  $\bar{x}_{(\text{SOA})}$  were lower for the Chinese participants. This difference between speaker types could be due to multiple factors, including cultural and personal history differences that would need to be evaluat-

ed in future studies. This is part of the issue observed with many unidimensional task-dependent measurements, and a good example of where task-dependent measurements can provide obfuscated results.

### **Multifractal spectra as task-independent measure of complexity.**

The multifractal spectrum did capture a task independent look at the complexity in the system. Both  $f_{(\alpha)}$  and  $\alpha$  were stable over time and culture, reflecting that complexity is a task-independent measurement.  $f_{(\alpha)}$  did not appear to reflect much change for any participant, making it relatively inefficient in this particular task. Changes in  $\alpha$  were sufficient to differentiate between cognitive load measurements, making it at least as efficient as linear analysis. Its task-independent properties further push complexity ahead as an analytic tool.

**Holder.** As the task became more familiar, the Holder exponent generally became more orderly. Once the level of chaos decreased to a point where the system was too easy, the participant adjusted the parameters naturally and increased the complexity. This natural adjustment is represented as a rapid change in SOA or accuracy for the block in which the change occurs.

**Self-Organized Criticality.** Looking at the multifractal spectrums one can also see that the overall multifractal spectrum shape forms a hook with the  $D_{(\infty)}$  approximately  $2/3$  up the y-axis and  $D_{(-\infty)}$  drops below the x-axis indicating that it trends to infinity. This hook form is the same pattern one would expect from a Cantor set (as shown in Halsey et al (1986)) indicating that the participant is splitting the screen in half until the stimulus was discovered. This pattern could be modeled as a singular point attractor in a system.

**Task difficulty operationalized as task complexity**

Observations in the multifractal spectrum show that as the task became less difficult for the participant, the system generally became more orderly. This process continued until the SOA adjusted enough for the difficulty to rise adding more complexity to the system. These findings show that task difficulty is coupled with complexity. Further, even though complexity proved to be task-independent, difficulty seemed to change as a function of stimulus and culture.

**Cognitive load re-conceptualized as task complexity**

This increase in difficulty also increased the cognitive load on the system. Cognitive load is related to task difficulty and subsequently results in increased complexity measurements. Although cognitive load seems to be task dependent, it is different for everyone. Complexity seems to be task independent, making it a more efficient measurement of the system.

**Broader impacts (NSF, etc.)**

This study has many broader impacts, including implications in training programs and standardization of system complexity across scientific studies. Another use for this measure could be to distinguish differences between cognitive systems and better streamline task model conceptualization. With how close this task was to being a monofractal signal, it is not likely that it was an interaction between systems, indicating a much closer relationship between visual object recognition and motor control than previously suspected. Future studies could focus on other dual-sensory interactions using much the same process to establish complexity indexes for various systems.



## References

- Abraham, F., Abraham, R., & Shaw, C. (1990). *A Visual Introduction to Dynamical Systems Theory for Psychology*. Santa Cruze, CA: Aerial Press inc.
- Abraham, R., & Shaw, C. (1992). *Dynamics: The Geometry of Behavior* (2 ed.). (R. Devaney, Ed.) Redwood City, CA: Addison-Wesley Publishing Company.
- Andersson, G., Hagman, J., Talianzadeh, R., Svedberg, A., & Larsen, H. C. (2002). Effect of cognitive load on postural control. *Brain research bulletin*, 58(1), 135-139.
- Ashenfelter, K. T., Boker, S. M., Waddell, J. R., & Vitanov, N. (2009). Spatiotemporal symmetry and multifractal structure of head movements during dyadic conversation. *Journal of Experimental Psychology: Human Perception and Performance*, 35(4), 1072.
- Bak, P. (1996). *How Nature Works: The Science of Self-organized criticality*. New York, NY: Copernicus.
- Bogacz, R., Wagenmakers, E. J., Forstmann, B. U., & Nieuwenhuis, S. (2010). The neural basis of the speed–accuracy tradeoff. *Trends in neurosciences*, 33(1), 10-16.
- Bracewell, R. N. (1986). *The Fourier transform and its applications*. (2 ed.). New York, NY: McGraw-Hill.
- Chandler, P., & Sweller, J. (1991). Cognitive Load Theory and the Format of Instruction. *Cognition and Instruction*, 8(4), 293-332.

- DeLeeuw, K. E., & Mayer, R. E. (2008). A comparison of three measures of cognitive load: Evidence for separable measures of intrinsic, extraneous, and germane load. *Journal of Educational Psychology, 100*(1), 223-234.
- Donders, F. C. (1969). On the speed of mental processes. *Acta psychologica, 30*, 412-431.
- Douc, R., Moulines, E., & Stoffer, D. (2014). *Nonlinear Time Series: Theory, Methods and Applications with R Examples*. Boca Raton , FL: CRC Press.
- Festman, Y., Adam, J. J., Pratt, J., & Fischer, M. H. (2013). Both hand position and movement direction modulate visual attention. *Frontiers in psychology, 4*, 657. Epub.
- Frein, S. T., Jones, S. L., & Gerow, J. E. (2013). When it comes to Facebook there may be more to bad memory than just multitasking. *Computers in Human Behavior, 29*(6), 2179-2182.
- Ginns, P. (2006). Integrating information: A meta-analysis of the spatial contiguity and temporal contiguity effects. *Learning and Instruction, 16*, 511-525.
- Greenwald, A. G., McGhee, D. E., & Schwartz, J. L. (1998). Measuring individual differences in implicit cognition: the implicit association test. *Journal of personality and social psychology, 74*(6), 1464-1480.
- Halsey, T. C., Jensen, M. H., Kadanoff, L. P., Procaccia, I., & Shraiman, B. I. (1986). Fractal measures and their singularities: the characterization of strange sets. *Physical Review A, 33*(2), 1141-1152.
- Harley, T. A. (2013). *The psychology of language: From data to theory*. (4 ed.). New York, NY: Psychology Press.



- Kleinow, H. D. (2002). Testing Continuous Time Models in Financial Markets (Doctoral dissertation, Humboldt-Universität zu Berlin).
- Lyra, M. L., & Tsallis, C. (1998). Nonextensivity and multifractality in low-dimensional dissipative systems. *Physical review letters*, 80(1), 53-69.
- Macmillan, N. A. (2002). Signal Detection Theory. In S. S. Stevens, *Steven's Handbook of experimental psychology*. (3 ed., Vol. 4, pp. 43-90). New York: John Wiley & Sons, Inc.
- Mallat, S. (2009). *A Wavelet Tour of Signal Processing: The Sparse Way* (3 ed.). Burlington, MA: Academic Press.
- Mallat, S., & Hwang, W. L. (1992). Singularity detection and processing with wavelets. *IEEE Transactions on Information Theory*, 38(2), 617-643.
- Mandelbrot, B. B. (1983). *The fractal geometry of nature*. Macmillan.
- Paas, F. G., Van Merriënboer, & Jeroen, J. G. (1993). The efficiency of instructional conditions: An approach to combine mental effort and performance measures. *Journal of the Human Factors and Ergonomics Society*, 35(4), 737-743.
- Posner, M. I. (2005). Timing the Brain: Mental Chronometry as a Tool in Neuroscience. *PLoS Biology*, 3(2), e51.
- Robinson, P. (2001). Task complexity, task difficulty, and task production: Exploring interactions in a componential framework. *Applied linguistics*, 22(1), 27-57.
- Setz, C., Arnrich, B., Schumm, J., La Marca, R., Troster, G., & Ehlert, U. (2010). Discriminating Stress From Cognitive Load. *IEEE Transactions on Information Technology in Biomedicine*, 14(2), 410-417.

- Shumway, R., & Stoffer, D. (2011). *Time Series Analysis and its Applications: With R Examples* (3 ed.). New York, NY: Springer.
- Spruyt, A., Hermans, D., Houwer, J. D., & Eelen, P. (2003). On the nature of the affective priming effect: Affective priming of naming responses. *Social Cognition, 20*(3), 227-256.
- Sternberg, S. (1969). The discovery of processing stages: Extensions of Donders' method. *Acta psychologica, 30*, 276-315.
- Strang, G. (1993). Wavelet transforms versus Fourier transforms. *Bulletin of the American Mathematical Society, 28*(2), 288-305.
- Sun, Q., & Tang, Y. (2002). Singularity analysis using continuous wavelet transform for bearing fault diagnosis. *Mechanical systems and signal processing, 16*(6), 1025-1041.
- Sweller, J. (1988). Cognitive Load During Problem Solving: Effects on Learning. *Cognitive Science, 12*, 257-285.
- Sweller, J., Merriënboer, J. J., & Paas, F. G. (1998). Cognitive Architecture and Instructional Design. *Educational Psychology Review, 10*(3), 251-296.
- Walczyk, J. J., Igou, F. P., Dixon, A. P., & Tcholakian, T. (2013). Advancing lie detection by inducing cognitive load on liars: a review of relevant theories and techniques guided by lessons from polygraph-based approaches. *Frontiers in psychology, 4*, 14.
- Walker, J. S. (2008). *A primer on wavelets and their scientific applications*. (2 ed.). Boca Raton, FL: CRC press.

Wickelgren, W. A. (1977). Speed-accuracy tradeoff and information processing dynamics. *Acta psychologica*, 41(1), 67-85.

## Appendix A

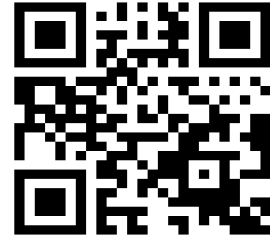
### Other Stuff



The folder with all the charts and graphs can be found here.



The program and a copy of my CV can be found at <http://1drv.ms/1cEYNZC>



The full dataset can be located at this location

**Thesis Summary Document:****Primary Motor Cortex Stimulation Affects Guidance**

**Statement of the Problem or Issue:** People observe objects close to their hands more efficiently than objects further from their hands. This occurs even when the hand is not visible, for example, when a person is talking on a cell phone and driving. Further knowledge about how this process works, and how one can measure it, could be useful in safer driving laws, better instrument panel layout, and the construction of more intuitive electronic devices.

**Brief Summary of the Literature:** Conceptually, cognitive load is the strain put on mental mechanisms during performance or schema creation. Researchers often give people a repetitive task and measure the decline in performance as task difficulty increases to study cognitive load. Heavy cognitive load has negative task performance effects, no matter the type, and the cognitive load experience differs from person to person. The choices for analyzing cognitive load performance data are often problematic as they are task-dependent and do not generalize well. This makes research into task-independent variables necessary. Complexity is one such measure that can be retrieved from normal cognitive load measures. Using time series analysis techniques provides a more efficient, and less altered route to measurements that can account for multiple task-dependent measures without being attached to the specific task.

**Thesis Statement:** Cognitive load can be operationalized as an individual's multifractal spectrum and measured using complexity.

**Statement of the Research Methodology:** Nonlinear time series analysis, more specifically I used wavelet transform modulus maxima to analyze a continuous wavelet

transform created from a time series based off the effect hand location has on object perception.

**Brief Summary of Findings:** We found that cognitive load can be operationalized as an individual's multifractal spectrum and measured using complexity. We also found evidence of visual search being a self-organizing critical system.

**Confirmation, Modification, or Denial of Thesis:**

**Statement of the Significance of the Findings:** SPSS was not analytically adequate for time series analysis. To circumvent this, I used the Continuous Wavelet Transform (CWT) method along with Wavelet Transform Modulus Maximus (WTMM) to extract the Holder exponents ( $\alpha$ ) from the system. Using these Holder exponents as a power law exponent I was able to use to extract the fractal dimensionality and create a multifractal spectrum. This view allowed for easy detection of system complexity at differing times during the learning process.

**Suggestions for Future Research:** In future studies it is advisable to use a 240<sub>Hz</sub> monitor. Moving forward from this location it would be interesting to use a continuous scale to determine hand location under the monitor. In this scenario, it would be necessary to save user profiles in order to have exact SOA's set for each location on the monitor at the blocks beginning.